

Modelling the temporal evolution of innovation statistics

Erik Andersson

ECMWF, Reading, U.K.

1. Introduction

In data assimilation an updated analysis of the atmospheric state is obtained by combining current information, that is, the most recent observations, with background information provided by a short-range forecast. Effectively, the background carries forward in time some of the information obtained from earlier assimilated observations. In operational numerical weather prediction, errors in the background and in the observations are of similar magnitude (Simmons 2003, these proceedings), which means that the observations can quite accurately be predicted, based on the information in the background. The difference vector between the predicted and the actual observations provide the *new information* to the analysis – these differences are called *innovations* (Daley 1991).

Innovations are non-zero either because of errors in the prediction or errors in the observations. The prediction errors are due to errors in the background (initial condition error) and to errors in the forecast model (model error). The observation errors depend on observation type, and is defined to include the errors of representativity. It is the job of the assimilation scheme to attribute the appropriate fractions of the innovations to the various error sources. This is done based on knowledge about the statistical characteristics of the errors involved, which is modelled and specified in the assimilation scheme. An accurate statistical model for the innovation error covariance is essential for good performance of any data assimilation scheme.

In three-dimensional assimilation schemes (Optimum Interpolation and 3D-Var), the simplification is made that the temporal aspects of innovation modelling can be ignored. In that case the modelling of innovations consists in a background-error covariance model (Fisher 2003, these proceedings) and the specified observation error covariances, respectively. Their magnitudes determine the relative weight given to the observations and the background in the analysis. In four-dimensional assimilation schemes (EnKF, Evensen 2003 and 4D-Var, Rabier 2003, these proceedings) the evolution of forecast error within the assimilation time window (12-hours in the ECMWF implementation, Bouttier 2001a) is accounted for. The modelled innovation covariance in that case incorporates the temporal variation. This enables effective assimilation of time-series of data (Järvinen et al. 1999), and data distributed frequently in time (Andersson et al. 2002). In the current study we investigate the temporal aspects of innovation covariances (Järvinen 2001) and compare actual innovation statistics with modelled innovation covariances within 4D-Var. We use hourly data from frequently reporting observing systems (aircraft, wind profilers, synop/ship and buoys) in regions with relatively uniform data coverage (North America, and North Atlantic).

After a brief description of the incremental formulation of 4D-Var in the next section (Section 2) we recapitulate (in Section 3) some of the earlier results provided by Järvinen's (2001) study of innovation time sequences. In Section 4 we describe innovation modelling within 4D-Var, focusing on the temporal aspects. Results from a comparison between actual and modelled innovations, for hourly data within the 12-hourly assimilation window, are presented in Section 5. Results are discussed and conclusions drawn in Section 6.

2. Incremental formulation of 4D-Var

The 4D-Var estimation problem is solved by minimising iteratively a cost function J with respect to the model state \mathbf{x} at the time t_0 at the start of the assimilation window. In the *incremental* formulation (Courtier *et al.* 1994) the cost function is written in terms of increments $\delta\mathbf{x}$ with respect to the background-state \mathbf{x}_b (a short-range forecast), i.e. $\delta\mathbf{x} = \mathbf{x} - \mathbf{x}_b$. The increments are propagated in time using the tangent linear $\mathbf{M} \equiv (\partial M / \partial \mathbf{x})|_{\mathbf{x}=\mathbf{x}_b}$ of the model M , and compared with the observations by means of the tangent linear \mathbf{H} of the observation operators H :

$$J(\delta\mathbf{x}) = \delta\mathbf{x}^T \mathbf{B}^{-1} \delta\mathbf{x} + \sum_{i=1}^N (\mathbf{H}_i \mathbf{M}_i \delta\mathbf{x} - \mathbf{d}_i)^T \mathbf{R}^{-1} (\mathbf{H}_i \mathbf{M}_i \delta\mathbf{x} - \mathbf{d}_i) \quad (1)$$

where the summation is over N sub-divisions (or *time slots*) of the assimilation time window. The length of each time slot was one hour (i.e. $N = 13$) in the operational system before January 2002 when it was halved to 30 minutes ($N = 25$). The vector \mathbf{d}_i represents the innovations:

$$\mathbf{d}_i = \mathbf{y}_i - H_i \mathbf{x}_b(t_i) = \mathbf{y}_i - H_i M_i \mathbf{x}_b(t_0), \quad (2)$$

where \mathbf{y}_i represents the observations. Note that the innovations are calculated using the non-linear observation operators, after propagating the model state to the time of the observations using the full non-linear forecast model at high resolution. This ensures the highest possible accuracy for the calculation of the innovations which are the primary input to the assimilation.

For computational cost reasons the increments $\delta\mathbf{x}$ are calculated at a lower resolution than that of the full model. The current forecast model is run at T511 spectral truncation (corresponding to a 40 km resolution) whereas the analysis increments $\delta\mathbf{x}$ are evaluated at T159 (120 km). The analyses $\mathbf{x}_a(t)$ at times $t = [0,6,12,18]$ UTC are formed by adding the increments to the background fields:

$$\mathbf{x}_a(t) = \mathbf{x}_b(t) + \delta\mathbf{x}(t). \quad (3)$$

3. Temporal evolution of innovations

In the study by Järvinen (2001) the temporal evolution of innovations was investigated within ECMWF's 3D and 4D-Var systems. North-American aircraft innovations for the period 1 September to 15 October 1997 were processed in hourly bins. The de-correlation method of Hollingsworth and Lönnberg (1986) was used to separate out the two contributions, observation and background error, from the innovations. Figure 1 shows the resulting hourly estimates of observation (cyan) and background errors (orange), alongside the specified values (blue and red, respectively), from a 6-hourly 3D-Var assimilation experiment (left) and 4D-Var (right). The estimated observation error (cyan) appears to be independent of time and independent of assimilation method, as expected. In 3D-Var the valid time of the background is the mid-time of the 6-hour window. The timing error due to the difference between the hourly data and the background shows clearly in the curve for estimated background error (orange). In 3D-Var an attempt is made to compensate for this variation by specifying larger observation errors (blue) for the off-time data - however, the specified values appear too large. The specified background error (red marker) at +3 hours is in good agreement with the estimated value at the centre of the assimilation window. The results for 4D-Var (right) are distinctly

different in terms of the background-error estimate (orange). In 4D-Var the background is valid at the initial time of the assimilation window (Rabier et al. 2000). The forecast model is used to propagate the background to the observation times, which inevitably introduces prediction errors increasing in time. The figure shows a significant growth of prediction error over the 6-hour period. It was also pointed out by Järvinen (*op. cit.*) that 4D-Var clearly outperforms 3D-Var, as the 4D-Var background error estimates are significantly lower than those for 3D-Var. It is therefore inappropriate to specify the same background errors in 4D and 3D-Var, and we can see that the specified error is too large in 4D-Var. Based on these and related results, both observation error and background errors were adjusted (with operational implementation in June 2000) and a better agreement between estimated and specified errors was achieved.

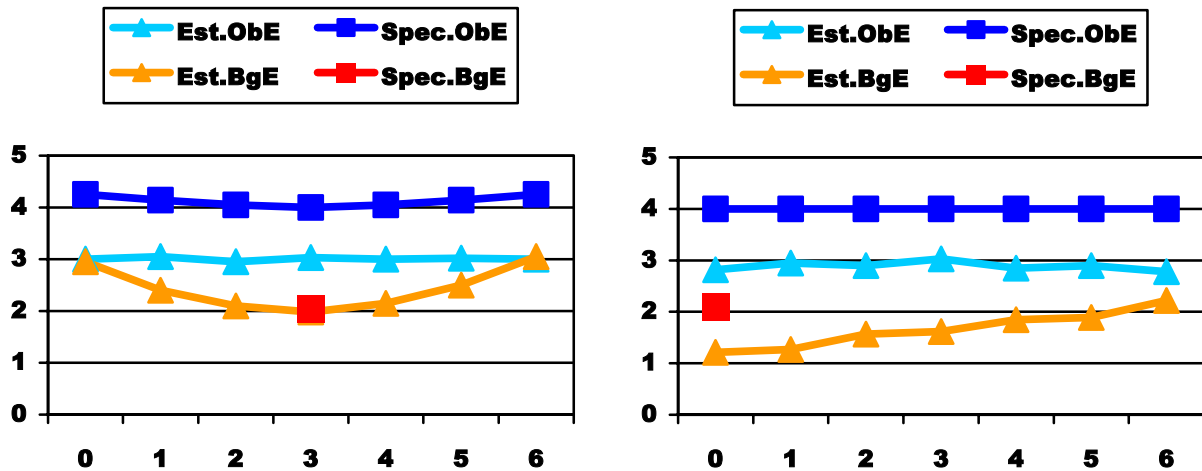


Figure 1 Evolution of background and observation errors (see legend) within 3D-Var (left) and 4D-Var (right) with a 6-hour assimilation window, for North American aircraft wind component (m s^{-1}) data. The estimated values (triangles) are obtained from actual innovation statistics for the period 1 September to 15 October 1997, processed in hourly bins. Specified values (square markers) are also shown, and refer to ECMWF's operational system in 1998. Adapted from Järvinen (2001).

The growth of prediction error is not uniform. Järvinen (2001) showed that the error growth is quickest for wind errors near jet-level (200 hPa), and relatively slower and more uniform in the vertical for temperature. His figure is reproduced here as Figure 2, showing vertical profiles of error at the beginning (thick dashed) and end (thin dashed line) of the 6-hour 4D-Var assimilation window. [The estimated observation error (full lines) is near constant in time (as expected).] The rapid error growth for wind near the jet level is reminiscent of singular-vector growth (Buizza and Palmer 1995). Singular vectors are characterized by rapid transfer of energy from potential to kinetic, and vertical propagation from the lower to the upper troposphere, within the first 6-12 hours of forecasts, due to baroclinic instability. In singular-vector growth there is a gradual shift from small to synoptic scales (Buizza 1998), which is another salient feature of short-range forecast error evolution.

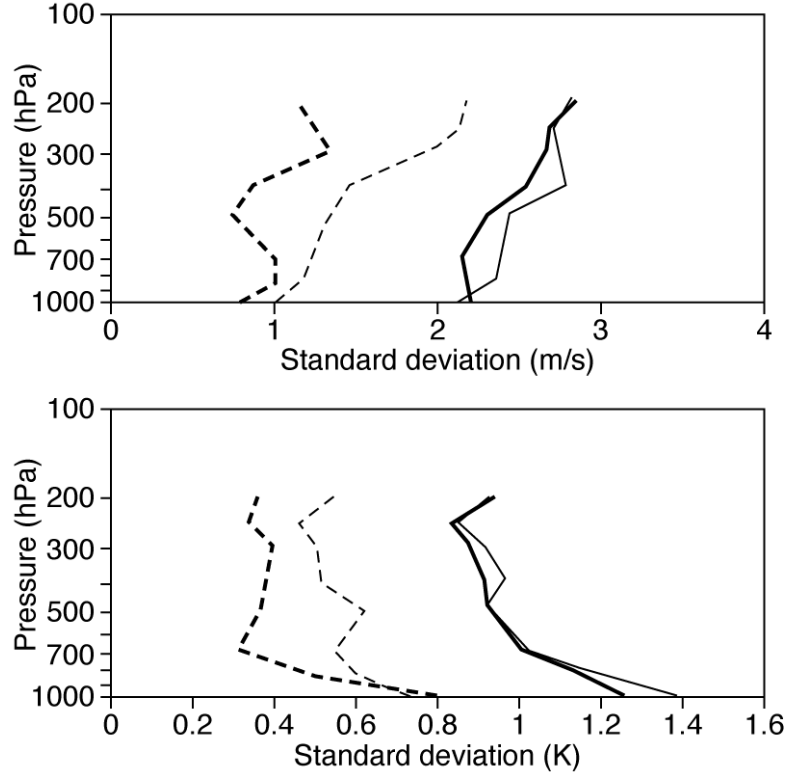


Figure 2 Vertical profiles of the background (dashed) and observation (solid line) error standard deviations at the beginning (thick) and end (thin line) of the 6-hour assimilation window, for aircraft component wind (top) and temperature (lower panel) data over North America, for the 4D-Var innovation sequence from 1 September to 15 October 1997. Reproduced from Järvinen (2001).

4. Modelling of innovation statistics

4.1. Error contributions

As mentioned in the Introduction, and can be seen from Eq.(2), the innovation vector is the difference between the observations and the model-equivalents of the observations. Apart from the observation vector and the background atmospheric state this also involves the forecast model and the observation operators. Unfortunately all four components of the calculation of the innovation vector are associated with errors, as defined in Table 1.

Table 1 Definition of errors ($\boldsymbol{\varepsilon}$) contributing to the innovation error covariance. The hat-symbol indicates 'true' values.

Definition	Expectation	Name
$\mathbf{y} = \hat{\mathbf{y}} + \boldsymbol{\varepsilon}_o$	$\langle \boldsymbol{\varepsilon}_o, \boldsymbol{\varepsilon}_o^T \rangle = \hat{\mathbf{O}}$	Observation error
$\mathbf{x}_b = \hat{\mathbf{x}}_b + \boldsymbol{\varepsilon}_b$	$\langle \boldsymbol{\varepsilon}_b, \boldsymbol{\varepsilon}_b^T \rangle = \hat{\mathbf{B}}$	Background error
$M\hat{\mathbf{x}}_{(t=0)} = \hat{\mathbf{x}}_{(t=T)} + \boldsymbol{\varepsilon}_q$	$\langle \boldsymbol{\varepsilon}_q, \boldsymbol{\varepsilon}_q^T \rangle = \hat{\mathbf{Q}}$	Model error
$H\hat{\mathbf{x}}_{(t)} = \hat{H}\hat{\mathbf{x}}_{(t)} + \boldsymbol{\varepsilon}_f$	$\langle \boldsymbol{\varepsilon}_f, \boldsymbol{\varepsilon}_f^T \rangle = \hat{\mathbf{F}}$	Representativity error

The four error contributions combine in the expression for the innovation error covariance (Dee 1995). Neglecting cross-correlations between observation and background we have:

$$\langle \mathbf{d}, \mathbf{d}^T \rangle = \hat{\mathbf{H}} \hat{\mathbf{P}}^f \hat{\mathbf{H}}^T + \hat{\mathbf{O}} + \hat{\mathbf{F}} \quad (4)$$

with

$$\hat{\mathbf{P}}^f = \hat{\mathbf{M}} \hat{\mathbf{B}} \hat{\mathbf{M}}^T + \hat{\mathbf{Q}} \quad (5)$$

where $\hat{\mathbf{P}}^f$ is *forecast error*, $\hat{\mathbf{M}} \hat{\mathbf{B}} \hat{\mathbf{M}}^T$ is *predictability error* and $\hat{\mathbf{Q}}$ is *model error*. The ‘hat’-symbol indicates ‘true’ values, in contrast to modelled values written without ‘hat’ in the following.

4.2. Simplifying assumptions

In 4D-Var, as in any other data assimilation scheme, the error covariances are modelled approximately. Approximations are unavoidable given the large dimension of the matrices involved (of the order $10^7 \times 10^7$ for \mathbf{B} , \mathbf{Q} and \mathbf{F} and $10^6 \times 10^6$ for \mathbf{O}). In the current ECMWF implementation of 4D-Var the following simplifying assumptions are made:

- Cross-correlation between observation and background are neglected,
- The observation errors are assumed un-correlated (diagonal $\mathbf{O} + \mathbf{F} = \mathbf{R}$), except temporal correlation of surface pressure data (Järvinen et al. 1999) which, however, we will disregard in the following,
- Zero model error ($\mathbf{Q} = 0$), that is, the perfect model assumption. Weak-constraint 4D-Var (i.e. $\mathbf{Q} \neq 0$) is also feasible (see Trémolet, 2003, these proceedings),
- The background error covariance (\mathbf{B}) is implemented as a chain of operators (Derber and Bouttier 1999), which together define the background-term (J_b), (Fisher 2003, these proceedings),
- The temporal evolution of the background-error covariance is provided by the tangent-linear (TL) forecast model (\mathbf{M}), at lower resolution. The TL model may or may not include representation of diabatic processes (Mahfouf 1999; Janisková et al. 2002). In this study an adiabatic TL model at T95 spectral triangular truncation was used,
- The conversion from model variables to observed quantities is performed with the tangent-linear of the observation operators (\mathbf{H}).

In summary, for 4D-Var we have:

$$\langle \mathbf{d}, \mathbf{d}^T \rangle = \mathbf{H} \mathbf{M} \mathbf{B} \mathbf{M}^T \mathbf{H}^T + \mathbf{R} \dots (+\mathbf{Q}) \quad (5)$$

In strong-constraint 4D-Var (e.g. ECMWF operations) $\mathbf{Q} = 0$. In ensemble Kalman Filters (EnKF, Houtekamer 2003, these proceedings) a rank- n estimate of the first right-hand-side term in Eq.(5) is obtained from the sample of n innovations available from the n ensemble members. For 3D-Var systems (Courtier et al. 1998) Eq.(5) simplifies to $\langle \mathbf{d}, \mathbf{d}^T \rangle = \mathbf{H} \mathbf{B} \mathbf{H}^T + \mathbf{R}$ (neglecting the temporal evolution, i.e. $\mathbf{M} = \mathbf{I}$), and in Optimum Interpolation (Lorenz 1981), where only very simple observation operators are possible (pure linear, or linearized around climatology, rather than the tangent-linear \mathbf{H} linearized around an accurate

background state), we have $\langle \mathbf{d}, \mathbf{d}^T \rangle = \mathbf{B}_o + \mathbf{R}$. In OI the background error covariance in terms of observed quantities (\mathbf{B}_o) is explicitly required (Lorenz 1986).

Given a sufficiently large sample of innovations, the left-hand side of Eq.(5) can be computed – at least the diagonal elements, that is, the innovation variances. Provided the diagonal elements of the right-hand side can also be evaluated then the actual and the modelled innovation variances can be inter-compared. This is recognised as an important validation step for any assimilation scheme. An accurate data assimilation procedure must model the innovations accurately in order to give the correct weight to the various observational data types and to the background. In 4D-Var and EnKF the temporal aspects come into play, determining the relative weight given to data at various times within the assimilation window, and extracting the appropriate tendency information and advective wind information from time-sequences of data. The first term on the right-hand side of Eq.(5) is not required explicitly in 4D-Var and cannot easily be inspected. However, the randomisation method suggested by Fisher and Courtier (1995), which previously has been used to diagnose the background error in terms of observable quantities (Andersson et al. 2000), i.e. \mathbf{HBH}^T , has in this paper been extended to include the model \mathbf{M} , thereby enabling Eq.(5) to be evaluated. The randomisation method for the term $\mathbf{HMBM}^T\mathbf{H}^T$ is described hereafter.

4.3. Computational aspects

Due to its definition (Fisher 2003, these proceedings) the 4D-Var control-variable χ is a standard multivariately normal quantity, i.e.:

$$\chi \sim \mathcal{N}(0, \mathbf{I}) \quad (6)$$

Any linear transformation of χ is also a normally distributed variable, with a different covariance. In particular for the increment in model space ($\delta\mathbf{x} = \mathbf{L}\chi$), we have (by virtue of the definition of \mathbf{L})

$$\mathbf{L}\chi = \delta\mathbf{x} \sim \mathcal{N}(0, \mathbf{B}) \quad (7)$$

and for the increment in terms of the observed quantity at observation time

$$\mathbf{HM}\delta\mathbf{x} \sim \mathcal{N}(0, \mathbf{HMBM}^T\mathbf{H}^T) \quad (8)$$

The covariances can be approximated through the following randomisation procedure: Generate a random sample of N vectors, $\chi^{(N)}$, with zero mean and unit variance, then

$$\chi^{(N)}(\chi^{(N)})^T \equiv \mathbf{I}^{(N)} \quad (9)$$

$$\mathbf{L}\chi^{(N)}(\mathbf{L}\chi^{(N)})^T \equiv \mathbf{B}^{(N)} \quad (10)$$

where $\mathbf{I}^{(N)}$ and $\mathbf{B}^{(N)}$ are rank- N approximations of the full matrices. Similarly a rank- N approximation of $\mathbf{HMBM}^T\mathbf{H}^T$ is obtained by applying the operators \mathbf{L} , \mathbf{H} and \mathbf{M} to each of the vectors $\chi^{(N)}$:

$$\mathbf{HML}\chi^{(N)}(\mathbf{HML}\chi^{(N)})^T \equiv \mathbf{HMBM}^T\mathbf{H}^T \quad (11)$$

Which is equivalent to

$$\mathbf{HMBM}^T \mathbf{H}^T \approx \frac{1}{N} \sum_{i=1}^N \mathbf{HML} \chi_i (\mathbf{HML} \chi_i)^T \quad (12)$$

For the purpose of this study we have evaluated Eq.(12) for a sample of $N=100$ vectors, accumulating variance contributions for the diagonal elements. The number of diagonal elements equal the total number of observations used in the current (October 2003) operational system, that is $\sim 3,500,000$ data. The uncertainty in the resulting individual variance estimates is $\sim 7\%$. The randomisation error is however negligible for accumulated statistics as presented in the following section.

5. Comparison between actual and modelled innovation time sequences

Using Eq.(12) we now have a practical method to evaluate Eq.(5), which enables us to carry out comparison between actual and modelled time-sequences of innovation variances. A mismatch can be due to any of a number of factors: The specified observation and background errors may be wrong, the tangent linear forecast model may be deficient in representing error growth, the observations may be affected by influences not fully described by the observation operators or by gross errors, and finally the neglect of model error may be damaging.

5.1. A fictitious example

For a well-tuned four-dimensional data assimilation system we might expect something like the picture shown in Figure 3. Note that this is a fictitious example, for illustration only, shown here to aid the discussion of the real results shown hereafter. Based on Järvinen's results (Section 3) the innovations (left) are expected to increase with time within the assimilation window (12 hours). The increase should ideally be matched (right panel) with a similar growth of forecast error, that is, predictability error (green) plus model error (red bars). The initial-condition error is represented by the green bar at time=0 in the right-hand panel. The observation error (light blue bars) provides a constant offset, independent of time.

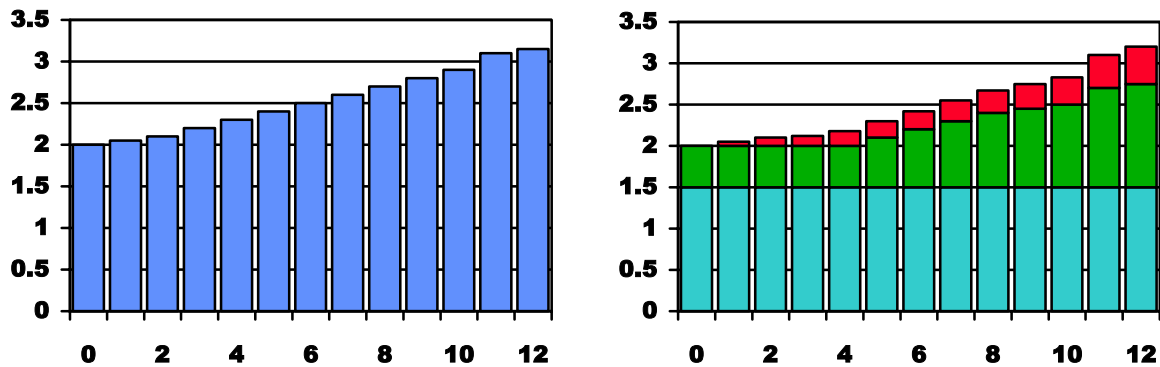


Figure 3 Expected result for a well-tuned four-dimensional data assimilation system: *fictitious data for illustration only*. Innovation statistics (left, blue bars) are compared with modelled statistics (right). The bars represent standard deviations (i.e. square-roots of the diagonal elements) of R (light blue), $R+HMBMH$ (green) and $R+HMBMH+Q$ (red), for each hour within the 12-hour assimilation window.

5.2. Results for frequent data in 4D-Var

A 4D-Var data assimilation experiment was carried out for the 6-day period from 12 UTC 20030205 to 12 UTC 20030211, using the version of the ECMWF forecasting system that was undergoing pre-operational testing at the time (cycle 26r3), and became operational in October 2003. A wide range of conventional and

satellite data was used (Thépaut 2003, these proceedings; Thépaut and Andersson 2003) and in particular hourly surface pressure data (Järvinen et al. 1999), frequent wind profiler (Bouttier 2001b; Andersson and Garcia-Mendez 2002) and frequent aircraft data (Cardinali et al. 2003). The diagonal elements (the innovation variances) of the left and the right-hand sides of Eq.(5) were evaluated for all available data (~3,500,000 per 12-hour period), and aggregated by observation type and by geographical area. The most stable statistics were obtained from regions with relatively homogeneous data coverage for the frequently reporting data types. Results are shown for jet-level (200-300 hPa) u-component wind data over North America (Figure 4) and for surface pressure data in the North Atlantic (Figure 5).

Figure 4 shows that the innovations (blue bars) clearly increase with time over the 12-hour period – more so for the sample provided by the wind-profiler network (top), than for the aircraft data (lower panels). The difference is most likely due to different sampling of the meteorological situation in the short study period, and the associated baroclinic and diabatic growth rates. The specified observation error (light blue) for both data types appear to be slightly over-estimated, as the observation error on its own is almost as large as the innovations are at time=0. The sum of initial condition error (green bar at time=0) and observation error is certainly overestimated, as this sum (in terms of variances) should equal the innovation variance at initial time. The most striking result is that the modelled forecast error evolution does not reproduce the error growth indicated by the innovations. In fact, for the first six or seven hours the modelled forecast error decreases, later followed by a weak increase. This result is surprising as it is expected that most of the error growth within the jet-level at mid-latitudes is due to baroclinic processes, which are well described by the TL forecast model.

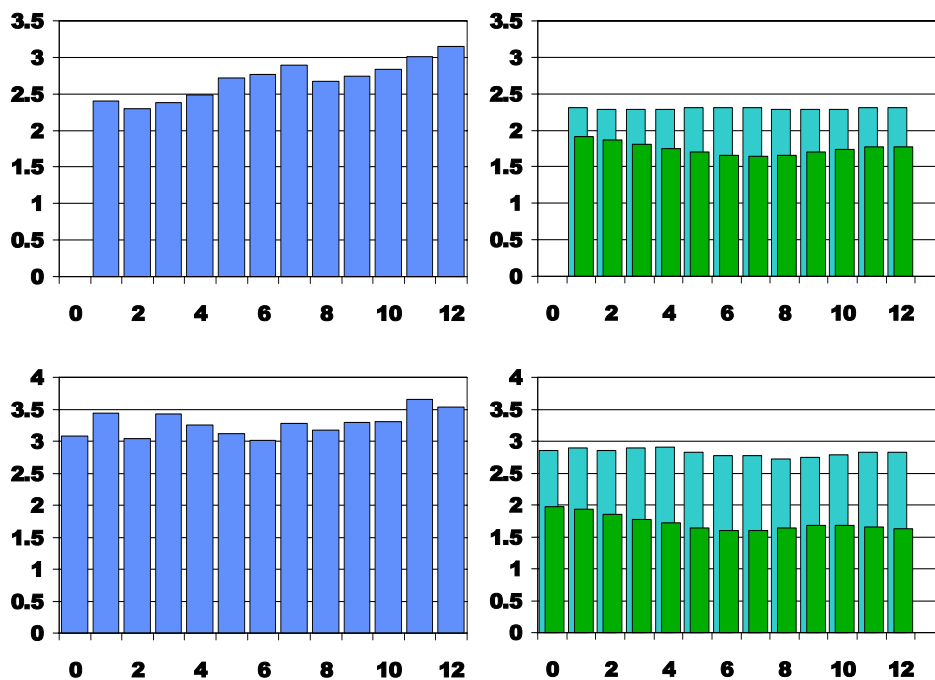


Figure 4 Innovation statistics based on actual data (left, blue bars) are compared against 4D-Var modelled innovations (right), for u-component wind data 200-300 hPa from American wind profilers (top), and aircraft over North America (lower panels), 20030205-12 to 20030211-12. The bars represent standard deviations (i.e. square-roots of the diagonal elements, ms^{-1}) of R (light blue) and HMBMH (green), for each hour within the 12-hour assimilation window.

In Figure 5 we show a similar set of diagrams, but this time for surface pressure data in the North Atlantic. Again, there is a clear indication that the innovations (blue) gradually increase over the 12-hour period. The

modelled error evolution, however, is almost flat (or decreasing) for the initial three to four hours, followed by a slow gradual increase. The sum of observation error and initial condition error is overestimated which is seen through comparison with the innovations at time=0. The observation errors should certainly be reduced, especially for SYNOP/SHIP data at the intermediate hours (when most data come from accurate automatic stations).

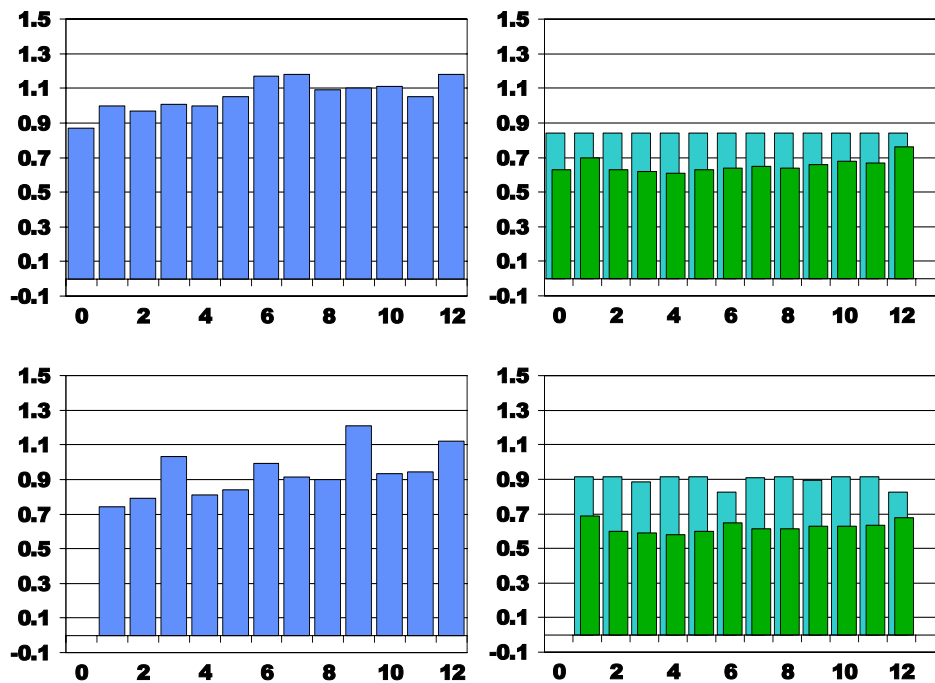


Figure 5 As Figure 4 for surface pressure data (hPa) in the North Atlantic from DRIBU (drifting buoy) (top) and SYNOP/SHIP (lower panels).

5.3. Discussion

The results shown here may at first seem contradictory to those of Thépaut et al. (1993, 1996) and Järvinen et al. (1999) who, in certain case studies, have demonstrated that 4D-Var generates flow-dependent structure functions and amplifies the error variance through evolution of the background error covariance matrix. They have shown that larger weight is given to data in the vicinity of dynamically active synoptic weather systems (see also Cardinali et al. 2003, these proceedings). Their results confirm that the background-error covariance is modified by growing baroclinic modes, within the assimilation period. It is nevertheless plausible that the balance between growing and neutral/decaying modes is incorrectly modelled, which could explain the results shown here and at the same time be compatible with those earlier results. In 4D-Var the covariance of initial-condition error is provided by the \mathbf{B} -matrix. The results shown here would suggest that the component of the variance in \mathbf{B} that projects onto growing modes is underestimated or that the decaying modes are overestimated. The investigations performed so far are insufficient to be able to be conclusive on this assumption.

There are other possibilities that could also explain the discrepancy between modelled and actual innovation evolution. One is that the tangent-linear forecast model could be deficient. In this study a low-resolution (T95) adiabatic TL model was used. It is possible that the inclusion of diabatic processes in the TL model (Janisková 2003, these proceedings) running at higher resolution (T159 or higher) will introduce more rapid and realistic growth rates. A third possibility is that model error is significant. It could be that the growth of

model error \mathbf{Q} is not as shown schematically in Figure 3, but much faster during the first few hours of forecasts and then saturates. The attempts that have been carried out so far, trying to quantify the model-error contribution to innovation statistics, have been unsuccessful because the uncertainties in the estimations of \mathbf{R} and \mathbf{B} dominate.

6. Conclusions

In this study we have compared the temporal evolution of actual innovations against those modelled within the ECMWF 4D-Var data assimilation system. Järvinen (2001) had shown that especially the wind innovation variances at jet-level grow quickly within the assimilation period (6-hours in his study). We have confirmed Järvinen's results for jet-level wind data over North America, and shown that also surface pressure innovations over the North Atlantic grow gradually over the assimilation period (12 hours in this study).

We developed a method to diagnose the evolution of the background error covariance within 4D-Var, including the transformation to observation-space using the adiabatic tangent-linear forecast model at T95 resolution and the tangent-linear observation operators. The method enables hourly comparison between the actual innovations and those modelled by 4D-Var. The comparison showed that there is an initial period of about 3-6 hours in which the modelled forecast error variance evolution either decreases or is near-constant in time, in clear contrast to the actual innovations. Later in the assimilation period (between 6 and 12 hours) the covariance evolution is showing error-growth, in better agreement with the innovations.

There are three possible explanations for the discrepancy:

1. The projection of the background-error covariance matrix onto the growing modes of the model is too small, or the projection on decaying modes is too large. Background error covariance models that explicitly assign a variance spectrum to the modes of the linear model have been constructed (Phillips 1986; Žagar et al. 2003). This approach is suitable for simplified linear models but less practical for primitive-equation models, especially if the domain extends into the upper stratosphere which is the case for the ECMWF model. Other approaches to include flow-dependent baroclinic structures into the B-matrix are discussed by Fisher (2003, these proceedings) and Fisher and Andersson (2001).
2. The low-resolution (T95) adiabatic tangent-linear model used in this study might be deficient in its representation of perturbation growth. Moist physical processes evolve much faster than baroclinic processes (Errico 1997) and may contribute significantly to perturbation growth within the first few hours of forecasts. Error-growth at scales beyond T95 would also contribute. In the final minimisation step of 4D-Var a diabatic tangent-linear model is used at T159 resolution, and parameterisations of moist physical processes are being incorporated (Janisková 2003, these proceedings). The impact of higher-resolution and the use of a diabatic TL model on the diagnostics presented here should be investigated.
3. The neglect of model error. Little is known about the magnitude and evolution of model error within the 12-hour assimilation window. It could be that model error grows very rapidly within the first few hours of forecasts and then saturates, which could at least partly explain the discrepancy seen here.

Other results of this study relate to error specification at initial time, that is \mathbf{B} and \mathbf{R} . From the small selection of results shown here it appears that specified observation errors for several observation types are too large, and should be reduced. Smaller observation error should be assigned to SYNOP/SHIP surface pressure data at intermediate hours (automatic stations) than at the synoptic hours (presumably manual stations).

Acknowledgements

The author wishes to thank François Bouttier (Météo-France), Carla Cardinali, Lars Isaksen and Sami Saarinen for developing and maintaining the ‘obstat’ observation-based data-assimilation diagnostic software, heavily used in this study. Colleagues in the Data Assimilation section at ECMWF are thanked for valuable discussions. Martin Ehrendorfer (U. of Vienna) provided the compact description of the randomisation method. Adrian Simmons provided helpful comments on the manuscript.

References

- Andersson, E., M. Fisher, R. Munro and A. McNally, 2000: Diagnosis of background errors for radiances and other observable quantities in a variational data assimilation scheme, and the explanation of a case of poor convergence. *Q. J. R. Meteorol. Soc.* **126**, 1455-1472.
- Andersson, E. and A. Garcia-Mendez, 2002: Assessment of European wind profiler data, in an NWP context. *ECMWF Tech. Memo.*, **372**, pp 14.
- Andersson, E., C. Cardinali, L. Isaksen and A. Garcia-Mendez, 2002: On the impact of frequent data in ECMWF's 4D-Var scheme: Hourly surface pressure data, European profilers and profiling aircraft data. Proc. 8th Workshop on "Meteorological Operational Systems", ECMWF, Reading, 12-16 November 2001, 179-183.
- Bouttier, F., 2001a: The development of 12-hourly 4D-Var. *ECMWF Tech. Memo.* **348**, pp 21.
- Bouttier, F., 2001b: The use of profiler data at ECMWF. *Meteorologische Zeitschrift*, **10**, 497-510.
- Buizza, R. and T.N. Palmer, 1995: The singular-vector structure of the atmospheric general circulation. *J. Atmos. Sci.*, **52**, 9, 1434-1456.
- Buizza, R., 1998: Impact of horizontal diffusion on T21, T42 and T63 singular vectors. *J. Atmos. Sci.*, **55**, 6, 1069-1083.
- Cardinali, C., L. Isaksen and E. Andersson, 2003: Use and impact of automated aircraft data in a global 4D-Var data assimilation system. *Mon. Wea. Rev.*, **131**, 1865-1877.
- Courtier, P., J.N. Thépaut and A. Hollingsworth, 1994: A strategy for operational implementation of 4D-Var, using an incremental approach. *Q. J. R. Meteorol. Soc.* **120**, 1367-1388.
- Courtier, P., E. Andersson, W. Heckley, J. Pailleux, D. Vasiljevic, M. Hamrud, A. Hollingsworth, F. Rabier and M. Fisher, 1998: The ECMWF implementation of three-dimensional variational assimilation (3D-Var). Part I: Formulation. *Q. J. R. Meteorol. Soc.* **124**, 1783-1807.
- Daley, R., 1991: *Atmospheric Data Analysis*, Cambridge University Press, pp 457.
- Dee, D. P., 1995: On-line estimation of error covariance parameters for atmospheric data assimilation. *Mon. Wea. Rev.*, **123**, 1128-1145.
- Derber, J.C. and F. Bouttier, 1999: A reformulation of the background error covariance in the ECMWF global data assimilation system. *Tellus*, **51A**, 195-221.
- Errico, R., 1997: What is an adjoint model? *Bull. Amer. Meteorol. Soc.*, **78**, 2577-2591.
- Fisher, M. and P. Courtier, 1995: Estimating the covariance matrices of analysis and forecast error in variational data assimilation. *ECMWF Tech. Memo.*, **220**, pp 26.
- Fisher, M. and E. Andersson, 2001: Developments in 4D-Var and Kalman Filtering. *ECMWF Tech Memo*, **347**, pp 36.

- Hollingsworth, A. and P. Lönnberg, 1986: The statistical structure of short-range forecast errors as determined from radiosonde data. Part I. The wind field. *Tellus*, **38A**, 111-136.
- Janisková, M., J.-F. Mahfouf, J.-J. Morcrette and F. Chevallier, 2002: Linearized radiation and cloud schemes in the ECMWF model: Development and evaluation. *Q. J. R. Meteorol. Soc.*, **128**, 1505-1527.
- Järvinen, H., 2001: Temporal evolution of innovation and residual statistics in the ECMWF variational data assimilation systems. *Tellus*, **53A**, 333-347.
- Järvinen, H., E. Andersson and F. Bouttier, 1999: Variational assimilation of time sequences of surface observations with serially correlated errors. *Tellus*, **51A**, 469-488.
- Lorenc, A.C., 1981: A global three-dimensional multivariate statistical interpolation scheme. *Mon. Wea. Rev.*, **109**, 701-721.
- Lorenc, A.C., 1986: Analysis methods for numerical weather prediction. *Q. J. R. Meteorol. Soc.*, **112**, 1177-1194.
- Mahfouf, J-F., 1999: Influence of physical processes on the tangent linear approximation. *Tellus*, **51A**, 147-166.
- Phillips, N., 1986: The spatial statistics of random geostrophic modes and first-guess errors. *Tellus*, **38A**, 314-322.
- Rabier, F., H. Järvinen, E. Klinker, J.F. Mahfouf and A. Simmons, 2000: The ECMWF operational implementation of four-dimensional variational assimilation. Part I: experimental results with simplified physics. *Q. J. R. Meteorol. Soc.* **126**, 1143-1170.
- Thépaut, J.N. and E. Andersson, 2003: Assimilation of high-resolution satellite data. *ECMWF Newsletter*, **97**, 6-12.
- Thépaut, J.N., R.N. Hoffman and P. Courtier, 1993: Interactions of dynamics and observations in a four-dimensional variational assimilation. *Mon. Wea. Rev.*, **121**, 3393-3414.
- Thépaut, J.N., P. Courtier, G. Belaud and G. Lemaître, 1996: Dynamical structure functions in four-dimensional variational assimilation: A case study. *Q. J. R. Meteorol. Soc.*, **122**, 535-561.
- Žagar, N., N. Gustafsson and E. Källén, 2003: Variational data assimilation in the tropics: the impact of background error constraint. *Q. J. R. Meteorol. Soc.*, In press.